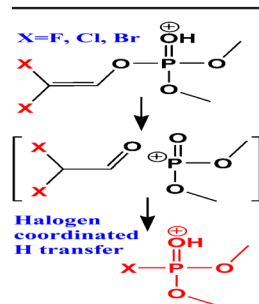**RESEARCH ARTICLE**

Intramolecular Halogen Atom Coordinated H Transfer via Ion-Neutral Complex in the Gas Phase Dissociation of Protonated Dichlorvos Derivatives

Xiaoping Zhang, Shuai Cheng

Jiangxi Key Laboratory for Mass Spectrometry and Instrumentation, East China University of Technology, Nanchang, 330013, People's Republic of China

Abstract. Intramolecular halogen atom coordinated H transfer reaction in the gas phase dissociation of protonated dichlorvos derivatives has been explored by electrospray ionization tandem mass spectrometry. Upon collisional activation, protonated dichlorvos underwent dissociation reaction via cleavage of the P–O bond to give reactive ion-neutral complex (INC) intermediate, [dimethoxylphosphinoylium + dichloroacetaldehyde]. Besides direct dissociation of the complex, intramolecular chlorine atom coordinated H transfer reaction within the complex takes place, leading to the formation of protonated dimethyl chlorophosphate. To investigate the fragmentation mechanism, deuterium-labeled experiments and several other halogen-substituted (Br and F) analogs of dichlorvos were prepared and evaluated, which display a similar intramolecular halogen transfer. Density functional theory (DFT)-based calculations were performed and the computational results also support the mechanism.

Keywords: Intramolecular halogen coordinated H transfer, Dichlorvos, Ion-neutral complex, Electrospray ionization-mass spectrometry

Introduction

Electrospray ionization-mass spectrometry (ESI-MS) combined with collision-induced dissociation (CID) has been proven to be invaluable for the investigation of gas-phase reactions [1–5] and to understand the detailed mechanisms of reactions in the condensed phase [6, 7]. Such fundamental studies are also important to underpin MS^n-based structure elucidation, which is challenged by rearrangement reactions [4, 8–28], such as proton transfer [20], electron transfer [28], hydride transfer [22], benzyl cation transfer [17], electrophilic aromatic substitution [23], and nucleophilic aromatic substitution [4].

Intermolecular and intramolecular halogen transfer is of particular interest in both solution chemistry and gas-phase chemistry, and thus has been investigated experimentally and

modeled theoretically [29–37]. In the solution phase, intermolecular halogen transfer reactions have been frequently found in organic synthesis where the halogen atom transfers in the form of a radical [32, 34, 37]. Several types of gas-phase F-atom transfer reactions of fluorinated compounds have been investigated by electron ionization mass spectrometry (EI-MS), which involves an F-atom "ring-walk" migration mechanism [35, 36]. Liu et al. have reported the F-atom migration from trifluoromethoxy group to indole or phenol ring in atmospheric pressure ionization mass spectrometry [31]. Dissociation of protonated halogen-substituted amines has been reported to occur intramolecular halogen transfer reaction in ESI-MS, which is achieved via an [amine/halonium ion] intermediate generated by cleavage of C–N bond of the precursor ion [29]. Picazas-Márquez et al. reported the gas-phase iodine transfer reaction in fragmentation of mono- and bis-haloethylphosphonates by gas chromatography mass spectrometry (GC-MS) [33]. Transfer of a chlorine atom has also been mentioned in gas-phase ion–molecule reaction of 2,2-*di*chlorovinyl *di*methyl phosphate (dichlorvos) by ion trap mass spectrometry (IT-MS) [30], but no detailed mechanism has been documented to our knowledge.

Correspondence to: Xiaoping Zhang; *e-mail:* zhangxpsunshine@163.com

Dichlorvos, a typical organophosphorus pesticide (OP), is widely used for agricultural activities because of its high insecticidal activity, low price, and relatively low environmental persistence [38–44]. However, the widespread use of dichlorvos in farming leads to its residues on vegetable, fruit skins, and even in groundwater, which cause great harm to human health and the environment [38–44]. MS technique has been used for the identification and structural characterization of dichlorvos [38, 40, 43]. Nevertheless, previous studies mainly focused on the determination and quantification of dichlorvos by liquid chromatography in conjunction with mass spectrometry (LC-MS) [43] and EI-MS [30, 45]. In this study, we present results from a detailed investigation on gas-phase fragmentation reactions of dichlorvos derivatives (Scheme 1), in which an intriguing rearrangement phenomenon involving halogen atom transfer was observed. Isotopic labeling experiments in conjunction with auxiliary theoretical calculations are carried out to support the proposed fragmentation mechanisms.
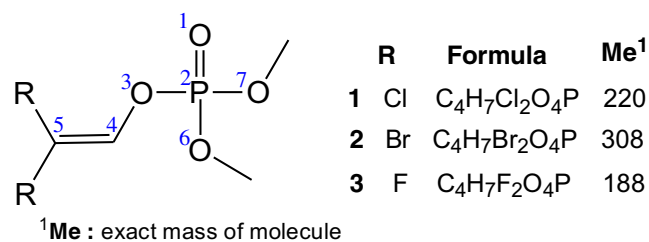
Experimental

Material and Methods

Methanol HPLC grade and methanol-$d4$ were purchased from Sigma-Aldrich (St. Louis, MO, USA) and Cambridge Isotope Laboratories, Inc. (Andover, MA, USA), respectively. Dichlorvos (compound **1**) and its derivatives (compounds **2** and **3**) were synthesized following reported procedures by reaction of trimethyl phosphite with the corresponding tri-halogenated (chloro-, bromo-, fluoro-) acetaldehydes, using the classic method (Scheme 1) [46]. The crude samples were analyzed directly by mass spectrometry after synthesis.

Mass Spectrometry

The samples were analyzed on an LTQ-XL advantage IT-MS equipped with an ESI interface in the positive ion mode (ThermoFisher, San Jose, CA, USA). Every diluted solution (1 μg mL^{-1} in methanol) was infused into the source chamber at a flow rate of 3 μL min^{-1}. The optimized ESI source conditions were as follows: ion-spray voltage, 3 kV; nebulizing gas (N$_2$), 25 arbitrary units (a.u.); capillary temperature, 150 °C, capillary voltage in 80 V; tube lens in 100 V. Other LTQ-XL parameters were automatically optimized by the system. The ion trap pressure of approximately 1×10^{-5} Torr was maintained with a Turbo pump, and pure helium (99.99%) was used as the collision gas. The CID-MS experiments were performed by using an excitation AC voltage to the end caps of the ion trap to include collisions of the isolated ions (isolation width at 1 Da) for a period of 30 ms and variable excitation amplitudes. The CID-MS spectra of the protonated molecules were obtained by activation of the precursor ions at the normalized collision energy of 20%.

Theoretical Calculations

Theoretical calculations were performed using the Gaussian 09 program [47]. The geometries of the target species were optimized using the density functional theory (DFT) method at the B3LYP/6-311+G(2d,p) level. The optimized structures were identified as a true minimum in energy by the absence of imaginary frequencies. Vibrational frequencies of all the key species were calculated at the same level of theory. The Cartesian coordinates of all structures involved are available as supplementary data. The energies discussed here are the sum of electronic and thermal free energy.

Result and Discussion

The gas-phase halogen atom transfer reaction was explored by investigating the MS fragmentation behavior of dichlorvos derivatives. Dichlorvos (compound **1**) was selected as a model to perform a detailed investigation. The CID mass spectrum of protonated dichlorvos $[\mathbf{1} + H]^+$ at m/z 221 is depicted in Figure 1a, in which three predominant peaks at m/z 109, m/z 127, and m/z 145 are observed. Formation of these ions has
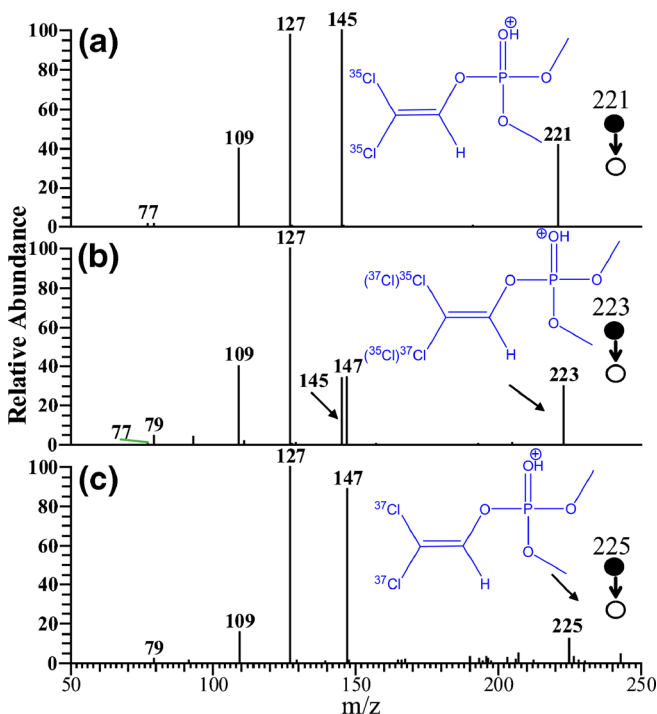

Figure 1. Collision-induced dissociation mass spectra of the $[M + H]^+$ ions of **(a)** 2,2-di^{35}chlorovinyl *di*methyl phosphate (m/z 221), **(b)** 2-^{35}chloro-2-^{37}chlorovinyl *di*methyl phosphate (m/z 223), and **(c)** 2,2-di^{37}chlorovinyl *di*methyl phosphate (m/z 225)

R	Formula	Me[1]
1 Cl	C$_4$H$_7$Cl$_2$O$_4$P	220
2 Br	C$_4$H$_7$Br$_2$O$_4$P	308
3 F	C$_4$H$_7$F$_2$O$_4$P	188

[1]**Me :** exact mass of molecule

Scheme 1. Structures of dichlorvos derivatives

been further consolidated by investigating the energy-resolved plots (see Supplementary Figure S1). The product ion at m/z 109 (**P1**, 39.8%) is ascribed to dimethoxylphosphinoylium, originating from the loss of $C_2H_2Cl_2O$ from the precursor ion (m/z 221). The ion at m/z 127 (**P2**, 98.1%) was assigned as the hydrated product of **P1**, which can be attributed to an ion–molecule reaction between the dimethoxylphosphinoylium at m/z 109 and residual water present in the vacuum system of ion trap [48]. Mass selection of the ion at m/z 109 directly results in the abundant ion at m/z 127 in the MS^3 experiment (see Supplementary Figure S2).

Here we are interested in the characteristic fragment ion marked as **P3** (100%) at m/z 145. **P3** is 76 Da less than the precursor ion corresponding to loss of C_2HClO, which can be assigned as the protonated dimethyl chorophosphate. Therefore, the formation of **P3** may be interpreted as a result of the transferring the chlorine atom from the carbon atom to the phosphorus atom, involving an interesting intramolecular halogen atom transfer reaction. To verify the proposed structure of **P3**, the MS^2 spectrum of protonated dimethyl chorophosphate was compared with the corresponding MS^3 spectrum of $[1 + H]^+$ (m/z 221 H$]m/z$ 145 →). As shown in Figure 2a, the MS^3 spectrum recorded from $[1 + H]^+$ at m/z 221 ion shows two main fragment ions at m/z 109 and m/z 127 by elimination of HCl, and subsequently associated H_2O, respectively. The MS^2 spectrum of protonated dimethyl chorophosphate (Figure 2b) displayed the same fragment ions with those from MS^3 spectrum of m/z 221, which verified that the structure of m/z 145 (P3) is protonated dimethyl chorophosphate. The ion at m/z 77 (**P4**) is also important (although less than 1%), resulting from the expulsion of dimethyl chlorophosphate (144 Da), which is a complementary ion of m/z 145.

The potential fragmentation pathways for the generation of **P1**, **P2**, **P3**, and **P4** from protonated dichlorvos are proposed in Schemes 2, 3, and Supplementary Scheme S1. The most
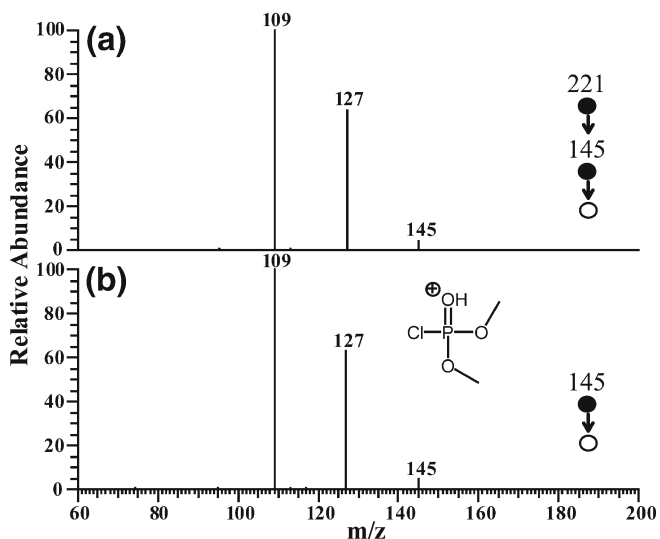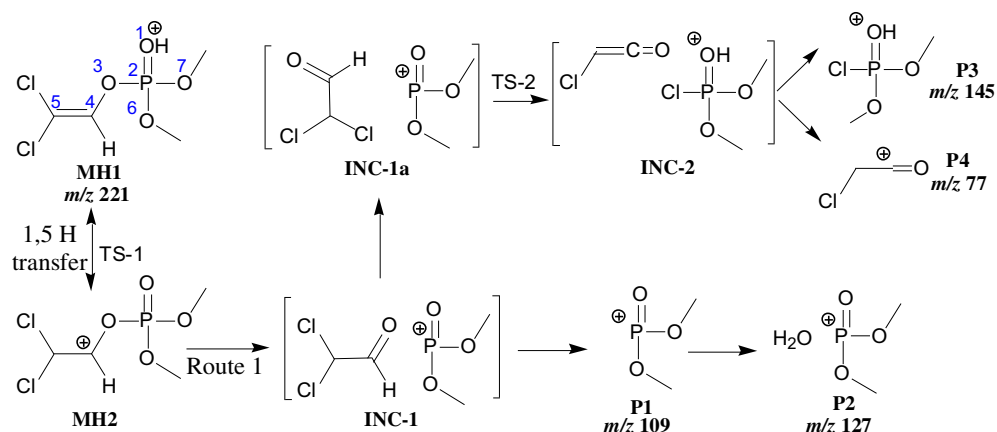
favored site of protonation for this compound is on the oxygen atom with high proton affinity [30] (will be discussed later). In route 1, the activated proton in **MH1** is transferred from the **O1** to the **C5** atom leading to an intermediate **MH2**, which triggers the subsequent dissociation to form an ion-neutral complex **INC-1** (dichloroacetaldehyde + dimethoxylphosphinoylium). A direct separation of **INC-1** results in the formation of **P1** at m/z 109, wereas an INC-mediated chloride and hydrogen transfer in **INC-1** lead to generation of **INC-2** (dimethyl chlorophosphate + chloro-ethenone), which undergoes the subsequent dissociation to afford **P3** at m/z 145 and **P4** at m/z 77. In route 2, the activated proton in **MH1** is transferred from the **O1** to the **C4** atom, leading to an intermediate **MH3**, which triggers the subsequent dissociation to form an ion-neutral complex **INC-3** (2,2-dichloro-oxirane + dimethoxylphosphinoylium). A direct separation of **INC-3** results in the formation of **P1** at m/z 109, whereas an INC-mediated chloride and hydrogen transfer in **INC-3** leads to generation of **INC-4**, which undergoes the subsequent dissociation to afford **P3** at m/z 145 and **P4** at m/z 77. In route 3, chloro atom may transfer from **C5** to **P2** directly via TS-4.

The proposed dissociation pathways in Schemes 2 and 3 were supported by the MS/MS analysis of the protonated ^{37}Cl isotopologue. No mass shift was observed for the product ion peaks of **P1** and **P2** in the fragmentation spectra of the native Cl-isotopologue of $[1 + H]^+$ at m/z 223 and m/z 225 (Figure 1b and c). This indicates that **P1** and **P2** do not contain the Cl atom. Interestingly, an increasing mass shift of 2 Da was observed for **P3** (from m/z 145 to m/z 147) in the fragmentation of the native ^{37}Cl-isotopologue of $[1 + H]^+$ at m/z 225 (two ^{37}Cl atom), which confirms that **P3** contains a ^{37}Cl atom originating from the ethylene moiety of the precursor ion (Figure 1c). Similarly, both fragment ions at m/z 145 and m/z 147 with abundance ratio of 1:1 were generated in the dissociation of the native ^{37}Cl-isotopologue of $[1 + H]^+$ at m/z 223 (^{37}Cl atom and ^{35}Cl atom). It also indicates that both the ^{35}Cl and ^{37}Cl atom on the **C5** can transfer to P atom with equal probability and form fragment ions at m/z 145 and m/z 147, respectively.

To better delineate the universality of the gas-phase halogen atom coordinated H transfer reaction, bromo-substituted and fluoro-substituted derivatives of dichlorvos (compounds **2** and **3**) were also investigated by tandem MS experiments. Figures 3 and 4 show the CID mass spectra of protonated 2,2-*di*bromovinyl *di*methyl phosphate and protonated 2,2-*di*fluorovinyl *di*methyl phosphate, respectively. Similar to the observed fragmentations of dichlorvos, the bromine coordinated H transfer product ion at m/z 189 (**P3**, $R_1 = {}^{79}Br$) and fluorine coordinated H transfer product ion at m/z 129 (**P3**, $R_1 = F$) can be observed clearly in Figures 3a and 4, respectively. No mass shift was observed for product **P1** (m/z 109) and its hydrated product **P2** (m/z 127). The relative abundance ratio of the halogenated **P3**/(**P1** + **P2**) product ions follows the order: 9.8 (R = Br) > 0.73 (R = Cl) > 0.25 (R = F), which is correlated to the relative C–X bond strengths (C-Br > C–Cl > C–F). The reason may be attributed to the C–Br bond's lower dissociation energy compared with those for the C–Cl and C–F bonds. A

Figure 2. **(a)** MS^3 spectrum of $[1 + H]^+$ (m/z 221 → m/z 145 →) and **(b)** MS^2 spectrum of protonated dimethyl chorophosphate (m/z 145 →)
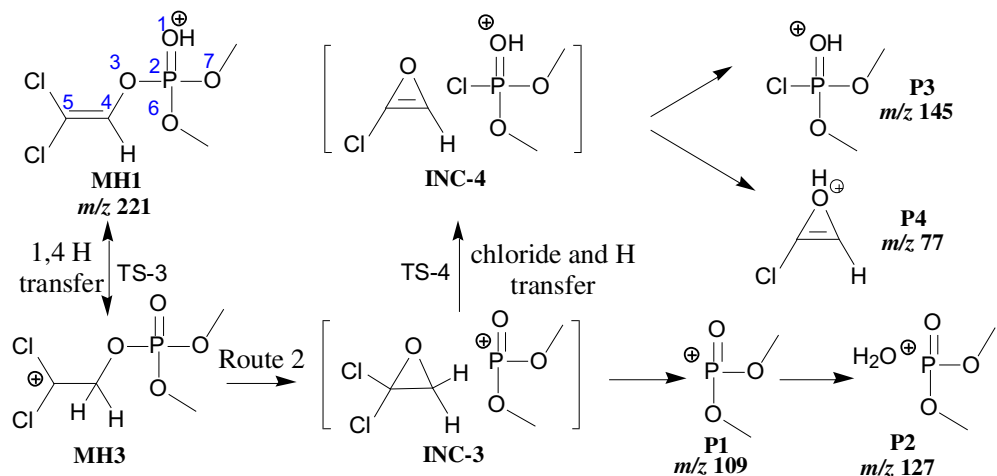
Scheme 2. Proposed reaction pathways of route 1 for the fragmentation of $[1 + H]^+$

minor peak at *m/z* 121 (**P4**, $R_2 = Br$) can also be observed in the dissociation of $[2 + H]^+$ (Figure 3a), resulting from the elimination of dimethyl bromophosphate (188 Da).

The dissociation of native Br-isotopologue of $[2 + H]^+$ display similar fragmentation patterns to those of $[1 + H]^+$ (Figure 3b and c). For example, fragment ions at *m/z* 189/191 and *m/z* 121/123 with abundance ratio of 1:1, respectively, are generated in the dissociation of the native ^{79}Br-isotopologue of $[2 + H]^+$ at *m/z* 311 (^{79}Br atom and ^{81}Br atom). However, significant differences except for corresponding **P1**, **P2**, and **P3** were found in the fragmentations of fluoro-substituted derivative of dichlorvos (Figure 4). As shown in Figure 4, a noticeable product ion at *m/z* 169 is observed, which involves the elimination of HF from $[3 + H]^+$ at *m/z* 189. The product ion *m/z* 169 may exist as a five-member ring structure, shown in Supplementary Scheme S1. Upon further dissociation, a transient intermediate (phosphene) at *m/z* 93 was formed by loss of oxo-acetyl fluoride from *m/z* 169 via a retro Diels-Alder reaction. The intermediate is easy to react with HF (originating from the formation of *m/z* 169), H_2O (residue in ion-trap). Thus, abundant ions at *m/z* 113 and *m/z* 131 can also be observed, derived from phosphene intermediate reacting with HF and HF + H_2O, respectively. The proposed **P4** ion at *m/z* 61

was not detected in the dissociation of $[3 + H]^+$, whereas an observable peak at *m/z* 81 is generated. The reason may be attributed to the ion/molecule reaction in the ion-trap, that is, the forming **P4** ion (*m/z* 61, $R_1 = F$) reacts with HF to generate product ion *m/z* 81. The possible fragmentation ways of $[3 + H]^+$ are depicted in Supplementary Scheme S1.

To provide insight into the mechanism of the halogen transfer reaction and explore the remarkable fragmentation differences among compounds **1**–**3**, density functional theory (DFT) calculations were carried out at the B3LYP/6-311++G(2d,p) level of theory. The protonation site is very important to the reaction mechanism. There are multiple protonation sites for dichlorvos (Scheme 1), including phosphoryl oxygen (**O1**), vinyl ether oxygen (**O3**), methoxy oxygen (**O6/O7**), and either carbon of the vinyl unit (**C4/C5**). The structures with different protonation sites of dichlorvos were optimized at the same level and the relative energies of these structures are summarized in Table 1. Overall, the calculation results indicate that **O1** atom is the most thermodynamically favorable protonation site, and it gives rise to **MH1** ion as described in Figure 1 and Scheme 2. It is often noted that fragmentation reactions take place when the proton transfers to other positions [5, 17]. That is, during the subsequent fragmentation process, the external proton has to

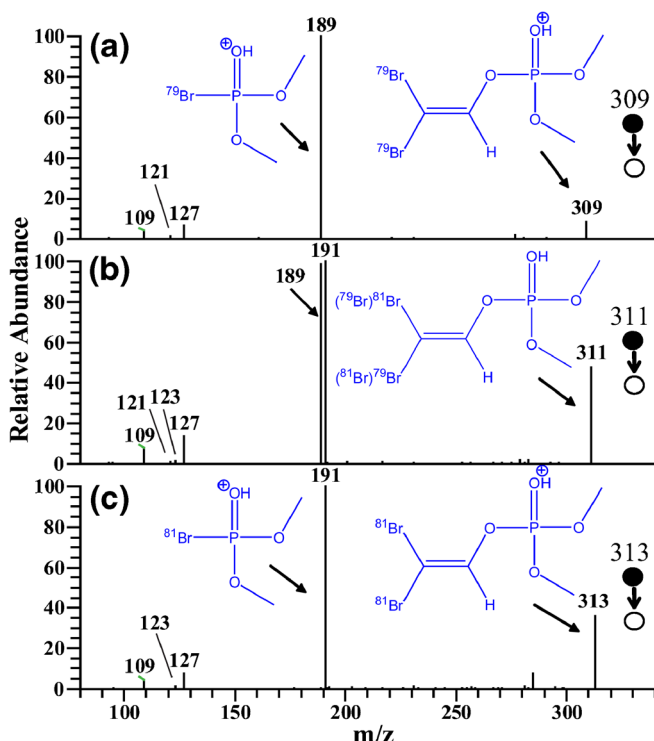**Scheme 3.** Proposed reaction pathways of route 2 for the fragmentation of $[1 + H]^+$

Figure 3. Collision-induced dissociation mass spectra of the [M + H]⁺ ions of **(a)** 2,2-di^{79}bromovinyl *di*methyl phosphate (*m/z* 309), **(b)** 2-^{79}bromo-2-^{81}bromovinyl *di*methyl phosphate (*m/z* 311), and **(c)** 2,2-di^{81}bromovinyl *di*methyl phosphate (*m/z* 313)

transfer via INC intermediate. Therefore, the concerted halogen transfer mechanism in route 3 can be excluded.

In the route 2, the proton may be transferred from **O1** to **C4** through a five-membered-ring transition state (**TS-3**), leading to the formation of **MH3** ion, which surmounts an energy barrier of 117.2 kJ mol⁻¹. This process is easily achieved in terms of energy. Unfortunately, the transition state (**TS-3a**) in this route could not be obtained despite great efforts. A potential energy surface scan on the **P2–O2** bond fixed from 1.67 Å to 3.87 Å with a stepsize of 0.03 Å shows consistent increase in energy during this process. Therefore, the activation energy needed should be close to **INC-3**. The sum free energies of the final product ion **P1** and 2,2-dichloro-oxirane are 233.6 kJ mol⁻¹ greater than that of **MH-1**, which suggested that this route is not favored from the perspective of energetics. In addition, the intermediate **INC-3** is also unstable with a high energy of 217.5 kJ mol⁻¹, so that this fragmentation pathway can also be excluded.

In route 1, the proton may be transferred from **O1** to **C5** through a six-membered-ring transition state (**TS-1**) first, leading to the formation of **MH2** ion, which surmounts an energy barrier of 151.9 kJ mol⁻¹. Interestingly, protonation at **C5** form **MH2** ion weakens the **P2–O3** bond, as indicated by the lengthened bond length (1.559 Å in **MH1** versus 1.849 Å in **MH2**, Figure 6). What we found from theoretical calculations is that once the external proton is attached to the **C5**, the **P2–O3** bond appears to dissociate spontaneously, and the two resulting fragments are still held together electrostatically as a stable **INC-1** with an energy of 58.9 kJ mol⁻¹.

INC is an important intermediate in gas-phase chemistry, and various chemical reactions can occur between the two species or in the ionic fragment alone prior to its final separation. Pan et al. reported that further reaction between the ion and the neutral species would occur if INC have suitable amount of internal energy [4]. The sum free energy of the separated ion **P1** and dichloroacetaldehyde is higher than that of **INC-1** by 85.8 kJ mol⁻¹; this indicates that **INC-1** seems relatively stable from the view of stabilization energy (the energy difference between ion-neutral complex and separation products). However, the minimum internal excess energy of **INC-1** is 93.0 kJ mol⁻¹ or at least 4.2 kJ mol⁻¹ above the separation energy, indicating a complex not very stable. Thus, direct separation of **INC-1** easily occurs in terms of energy,
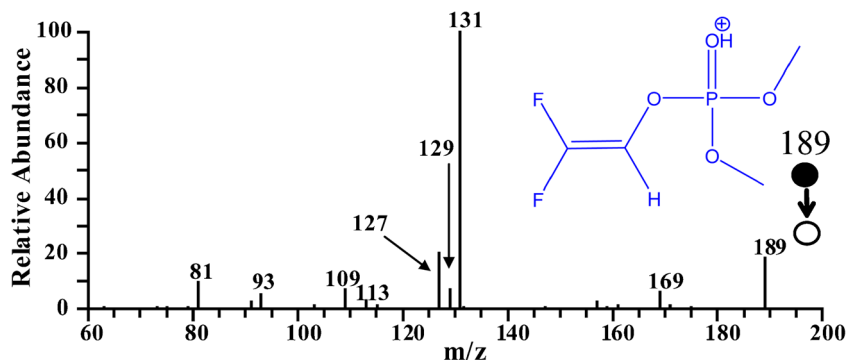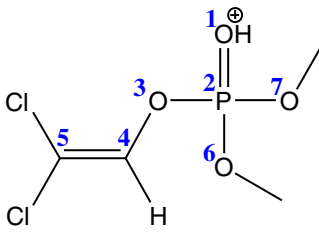
transfer from **O1** atom to other less favored sites. A schematic potential energy surface scan for the dissociation of [1 + H]⁺ is shown in Figure 5, and the key structures of relevant species are displayed in Figure 6 and the Supplementary Material (SupplementaryFigure S3).

From the calculation results, it can be found that the energy barriers in route 2 (red line) and route 3 (black line) are both significantly higher than that in route 1 (blue line). In route 3, the chloride atom may transfer directly from **C5** to **P2**, via a five-membered transition state **TS-4**. The mechanism can be viewed as a concerted C–Cl bond cleavage/P–O bond formation process. However, calculation results show that the transition state **TS-4** for the concerted mechanism is 133.3 kJ mol⁻¹ higher in free energy than the transition state for the stepwise

Figure 4. Collision-induced dissociation mass spectrum of the [M + H]⁺ ion of 2,2-*di*fluorovinyl *di*methyl phosphate (*m/z* 189)

Table 1. Relative Energies of $[1 + H]^+$ Ions with Different Protonation Sites

Compound **1**	Site of protonation	Relative energy (kJ mol^{-1})
	O1 of carbonyl oxygen	0.0
	O6/O7 of methoxy oxygen	111.9
	O3 of vinyl ether oxygen	111.1
	C4 of vinyl carbon	106.1
	C5 of vinyl carbon	58.9

which generates an abundance of ions of *m/z* 109 and *m/z* 127. In addition to direct separation to afford **P1** (*m/z* 109), the two species of **INC-1** can undergo rotation of structure to generate intermediate **INC-1a** via overcoming of a small energy barrier, which is indicated by the lengthened **C5**–Cl bond from 1.751 Å to 1.877 Å. The two partners in intermediate **INC-1a** can undergo migration of chlorine from **C5** to **P2** leading to the formation of **INC-2** via the transition state of **TS-2**, accompanied by migration of the hydrogen on **C4** to the **O1**. The energy barrier of **TS-2** is 63.8 kJ mol^{-1} higher than intermediate **INC-1a** in energy. It suggested that the chlorine atom transfer between the two partners within intermediate could be achieved.

The sum free energy of **P3** and chloro-ethenone is 3.8 kJ mol^{-1} less than that of the precursor ion (**MH1**), indicating that formation of **P3** is a thermodynamically favored process. The sum free energy of **P4** and dimethyl chlorophosphate is 63.9 kJ mol^{-1} more than that of **MH1**. However, the calculated stabilization energy of **INC-2** is –0.1 kJ mol^{-1}, suggesting that this structure is very unstable.
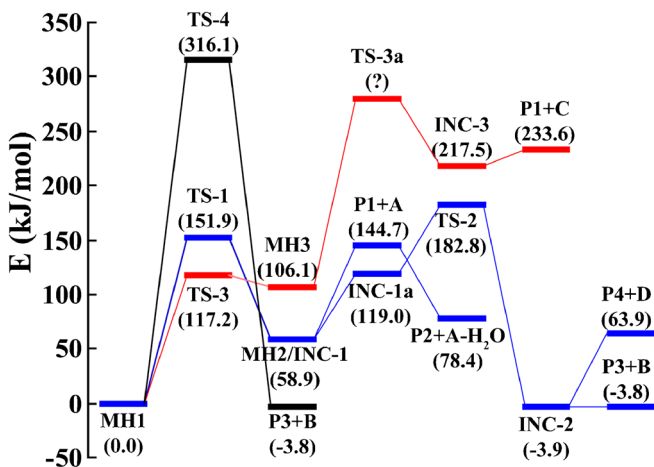

Figure 5. Potential energy diagram for $[1 + H]^+$. (**A**: dichloroacetaldehyde, **B**: chloro-ethenone, **C**: 2,2-dichloro-oxirane, **D**: dimethyl chlorophosphate)

Thus, the direct separation to form **P3** is the major path and the formation of **P4** is hard to occur.

The energy requirements for the direct separation products (**P1** + **A**) is 144.7 kJ mol^{-1} (product control), which is 38.1 kJ mol^{-1} lower than the energy barrier (**TS-2**, 182.8 kJ mol^{-1}) for the formation of **P3** and **P4** (transition state control). In addition, ion **P1** is easy to bind a water molecule to form ion **P2**; this process is exoergic by 66.3 kJ mol^{-1}. Thus, the sum intensities of ions **P1** and **P2** are higher than those of ions **P3** and **P4**, which is in good agreement with the CID experimental results (Figure 1a).

Similarly, the schematic potential energy surface scans for the dissociation of $[2 + H]^+$ and $[3 + H]^+$ are shown in the Supplementary Figures S4 and S5. According to our calculation results, it could be found that the key steps on the potential energy surface are altered by the change from chlorine to bromine or fluorine. For example, the energy barrier of **TS-1** and **TS-2** follows the order: 142.9 kJ mol^{-1} (R = Br) < 151.9 kJ mol^{-1} (R = Cl) < 164.1 kJ mol^{-1} (R = F) and 180.9 kJ mol^{-1} (R = Br) < 182.9 kJ mol^{-1} (R = Cl) < 184.4 kJ mol^{-1} (R = F), respectively; the energy of **INC-1** follows the order: 46.8 kJ mol^{-1} (R = Br) < 58.9 kJ mol^{-1} (R = Cl) < 62.9 kJ mol^{-1} (R = F). The energy barrier of **TS-2** (R = Br) is lower than that of **TS-2** (R = Cl or F).

What's more, in view of the competition between direct separation and halogen transfer being controlled by the stability of **INC-1**, the relative abundances of the two corresponding product ions change regularly depending on the variation in the stabilization energy of **INC-1**. For example, the calculated stabilization energy values follow the order: 97.6 kJ mol^{-1} (R = Br) > 85.8 kJ mol^{-1} (R = Cl) > 66.0 kJ mol^{-1} (R = F). The higher the stabilization energy, the easier the migration reaction between **INC-1** (**P3**), the harder the direct separation (**P1**). Thus, when R = Br, the sum abundance of **P3** and **P4** is higher than that of **P1** and **P2**, which is in accordance with the MS results.

Isotopic labeling is a powerful tool to explore reaction mechanisms, and thus a deuterium labeling experiment was carried out to further verify the theoretical calculation results (Figure 7). An abundant deuterated molecule $[1 + D]^+$ at *m/z* 222 was obtained by introducing a diluted methanol-d_4
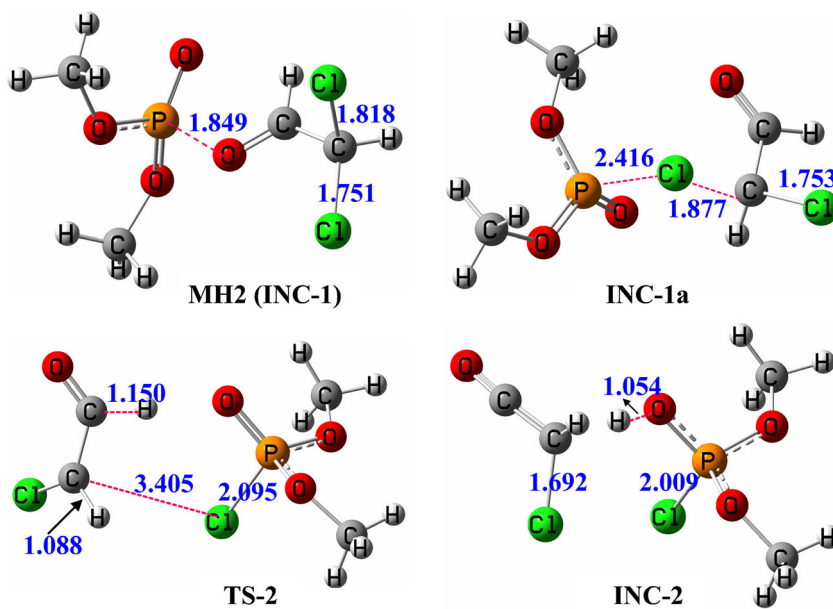
Figure 6. The optimized structures of key intermediates. The bond lengths are given in Å

solution of **1** for the positive MS analysis. There is no external proton in the fragment ions of **P1** and **P2**; therefore decomposition of $[1 + D]^+$ at *m/z* 222 resulted in the same mass (*m/z* 109 and *m/z* 127) as that of $[1 + H]^+$. The fragment ion **P3** contains a hydrogen atom, which may originate from the transfer of the hydrogen on **C4** atom. As expected, the corresponding mass at *m/z* 145 (not containing deuterium) was observed in the dissociation of $[1 + D]^+$. In addition, the observation of high abundance ion at *m/z* 146 indicated that the H/D exchange [49] reactions between the external deuterium and the hydrogen on **C4** may occur before dissociation (see Supplementary Scheme S3). Furthermore, the H/D exchange between **O1** and **C4**, through H migration via **TS-3**, only overcomes a small energy barrier of 117.2 kJ mol^{-1}, suggesting that this exchange reaction is easily achieved. H/D scrambling is also possible to occur at some point further along the potential energy surface after the formation of **INC-1** or **INC-2**. For example, according to the calculation results, after the formation of **INC-2**, the proton on the oxygen atom can transfer to the **C-5** atom. Similarly, the activated deuteron atom on the **C-5** may also transfer back to

the oxygen to form **INC-2-a**. The energy barrier for this H/D exchange process occurs easily, with a low energy barrier of −6.4 kJ mol^{-1}. However, the stabilization energy of **INC-2-a** is very low; thus it subsequently dissociates into **P3** (*m/z* 146) and **P4** (*m/z* 78). Also, H/D scrambling can also occur between **MD2-a** and **MD1-b** via 1,2 H/D transfer. A detailed process is displayed in Supplementary Scheme S3 below. In short, the deuterium labeling experiment is in accordance with the computational results.

Conclusion

In this study, an intriguing intramolecular halogen atom transfer reaction was observed in the gas-phase dissociation of protonated dichlorvos derivatives by electrospray ionization tandem mass spectrometry. D-labeled experiments and DFT calculations indicate convincing evidence that the halogen transfer was achieved via a [dimethoxylphosphinoylium + dichloroacetaldehyde] intermediate generated by proton
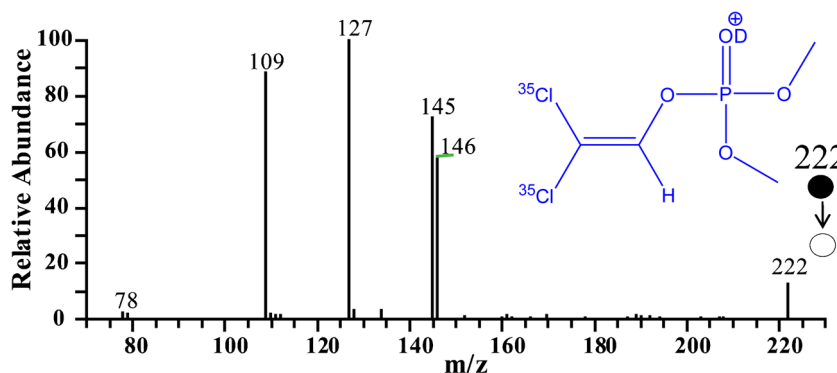

Figure 7. Collision-induced dissociation mass spectrum of the $[1 + D]^+$ ion at *m/z* 222

transfer and dissociation of the precursor ion via cleavage of the P–O bond, which is a stepwise transfer process. This study reports an interesting type of rearrangement reaction in the gas-phase chemistry, which can enrich our knowledge of the special gas-phase reactivity of halogenated organophosphorus esters and will provide valuable information in further analytical research of related compounds by mass spectrometry. Further work in this area will be performed in our laboratory.

Acknowledgements

References

1. Hopfgartner, G., Bourgogne, E.: Quantitative high-throughput analysis of drugs in biological matrices by mass spectrometry. Mass Spectrom. Rev. **22**, 195–214 (2003)
2. Longevialle, P.: Ion–neutral complexes in the unimolecular reactivity of organic cations in the gas phase. Mass Spectrom. Rev. **11**, 157–192 (1992)
3. Vukics, V., Guttman, A.: Structural characterization of flavonoid glycosides by multi-stage mass spectrometry. Mass Spectrom. Rev. **29**, 1–16 (2010)
4. Chai, Y., Jiang, K., Sun, C., Pan, Y.: Gas-phase nucleophilic aromatic substitution between piperazine and halobenzyl cations: reactivity of the methylene arenium form of benzyl cations. Chemistry **17**, 10820–10824 (2011)
5. Hu, N., Tu, Y.-P., Jiang, K., Pan, Y.: Intramolecular charge transfer in the gas phase: fragmentation of protonated sulfonamides in mass spectrometry. J. Org. Chem. **75**, 4244–4250 (2010)
6. Zhang, X., Bai, X., Fang, L., Jiang, K., Li, Z.: Decarboxylative coupling reaction in ESI(−)-MS/MS of 4-nitrobenzyl 4-hydroxybenzoates: triplet ion–neutral complex-mediated 4-nitrobenzyl transfer. J. Am. Soc. Mass Spectrom. **27**, 940–943 (2016)
7. Zhang, X., Jiang, K., Bai, X., Lv, H., Li, Z., Lee, M.R.: Observation of the intermediates of in-source aldolization reaction in electrospray ionization mass spectrometry analysis of heteroaromatic aldehydes. Eur. J. Mass Spectrom. **29**, 1102–1110 (2015)
8. Attygalle, A.B., Bialecki, J.B., Nishshanka, U., Weisbecker, C.S., Ruzicka, J.: Loss of benzene to generate an enolate anion by a site-specific double-hydrogen transfer during CID fragmentation of o-alkyl ethers of ortho-hydroxybenzoic acids. J. Mass Spectrom. **43**, 1224–1234 (2008)
9. Bialecki, J.B., Axe, F.U., Attygalle, A.B.: Hydroxycarbonyl anion (m/z 45), a diagnostic marker for α-hydroxy carboxylic acids. J. Mass Spectrom. **44**, 252–259 (2009)
10. Chai, Y., Gao, G., Shen, S., Liu, X., Lu, C.: Neutral losses of sodium benzoate and benzoic acid in the fragmentation of the [M + Na]⁺ ions of methoxyfenozide and tebufenozide via intramolecular rearrangement in

11. electrospray ionization tandem mass spectrometry. Rapid Commun. Mass Spectrom. **31**, 245–252 (2017)
11. Chai, Y., Wang, L., Wang, L.: How does a C=C double bond cleave in the gas phase? Fragmentation of protonated ketotifen in mass spectrometry. J. Mass Spectrom. **51**, 1105–1110 (2016)
12. Chen, Y., Le, D.C., Li, K., Cotham, W.E., Lee, N., Walla, M., Wang, Q.: A novel rearrangement of fluorescent human thymidylate synthase inhibitor analogues in ESI tandem mass spectrometry. J. Am. Soc. Mass Spectrom. **21**, 403–410 (2010)
13. Cyriac, J., Paulose, J., George, M., Ramesh, M., Srinivas, R., Giblin, D., Gross, M.L.: The role of methoxy group in the Nazarov cyclization of 1,5-bis-(2-methoxyphenyl)-1,4-pentadien-3-one in the gas phase and condensed phase. J. Am. Soc. Mass Spectrom. **25**, 398–409 (2014)
14. Edelson-Averbukh, M., Mandelbaum, A.: Intramolecular electrophilic aromatic substitution in gas-phase-protonated difunctional compounds containing one or two arylmethyl groups. J. Mass Spectrom. **38**, 1169–1177 (2003)
15. George, M., Sebastian, V.S., Reddy, P.N., Srinivas, R., Giblin, D., Gross, M.L.: Gas-phase Nazarov cyclization of protonated 2-methoxy and 2-hydroxychalcone: an example of intramolecular proton-transport catalysis. J. Am. Soc. Mass Spectrom. **20**, 805–818 (2009)
16. Greene, L.E., Grossert, J.S., White, R.L.: Correlations of ion structure with multiple fragmentation pathways arising from collision-induced dissociations of selected α-hydroxycarboxylic acid anions. J. Mass Spectrom. **48**, 312–320 (2013)
17. Guo, C., Yue, L., Guo, M., Jiang, K., Pan, Y.: Elimination of benzene from protonated N-benzylindoline: benzyl cation/proton transfer or direct proton transfer? J. Am. Soc. Mass Spectrom. **24**, 381–387 (2013)
18. Hibbs, J.A., Jariwala, F.B., Weisbecker, C.S., Attygalle, A.B.: Gas-phase fragmentations of anions derived from N-phenyl benzenesulfonamides. J. Am. Soc. Mass Spectrom. **24**, 1280–1287 (2013)
19. Hudson, C.E., Mcadoo, D.J.: Characterization by theory of H-transfers and onium reactions of CH₃CH₂CH₂N⁺H=CH₂. J. Am. Soc. Mass Spectrom. **18**, 270–278 (2007)
20. Jiang, K., Bian, G., Hu, N., Pan, Y., Lai, G.: Coordinated dissociative proton transfers of external proton and thiocarbamide hydrogen: MS experimental and theoretical studies on the fragmentation of protonated S-methyl benzenylmethylenehydrazine dithiocarboxylate in gas phase. Int. J. Mass Spectrom. **291**, 17–23 (2010)
21. Jiang, K., Zhang, H., Wang, J., Li, F., Qian, M.: Fragmentation of deprotonated diacylhydrazine derivatives in electrospray ionization tandem mass spectrometry: generation of acid anions via intramolecular rearrangement. PLoS One **8**, e63097 (2013)
22. Kuck, D.: Concomitant hydride and proton transfer: an essay on competing and consecutive key reactions occurring in gaseousin/neutral complexes. Eur. J. Mass Spectrom. **18**, 161–181 (2012)
23. Li, F., Zhang, X., Zhang, H., Jiang, K.: Gas-phase fragmentation of the protonated benzyl ester of proline: intramolecular electrophilic substitution versus hydride transfer. J. Mass Spectrom. **48**, 423–429 (2013)
24. Liu, J., Zhang, R., Jiuming, H.E., Liu, Y., Shi, J., Abliz, Z.: The characteristic fragmentation and rearrangement reaction of cationized glucopyranosyloxybenzyl tartrates by tandem mass spectrometry. J. Mass Spectrom. **45**, 824–828 (2010)
25. Paulose, J., Achuthan, R.P., Linsha, M.P.L., Mathai, G., Prasanth, B., Talluri, M.V.N.K., Srinivas, R.: Protonated N-benzyl- and N-(1-phenylethyl)tyrosine amides dissociate via ion/neutral complexes. Rapid Commun. Mass Spectrom. **29**, 1577–1584 (2015)
26. Rodriquez, C.F., Cunje, A., Shoeib, T., Chu, I.K., And, A.C.H., Siu, K.W.M.: Proton migration and tautomerism in protonated triglycine. J. Am. Chem. Soc. **123**, 3006–3012 (2001)
27. Wang, H.-Y., Xu, C., Zhu, W., Liu, G.-S., Guo, Y.-L.: Gas phase decarbonylation and cyclization reactions of protonated N-methyl-N-phenylmethacrylamide and its derivatives via an amide Claisen rearrangement. J. Am. Soc. Mass Spectrom. **23**, 2149–2157 (2012)
28. Wang, S., Guo, C., Zhang, N., Wu, Y., Zhang, H., Jiang, K.: Tosyl oxygen transfer and ion–neutral complex mediated electron transfer in the gas-phase fragmentation of the protonated N-phenyl p-toluenesulfonamides. Int. J. Mass Spectrom. **376**, 6–12 (2015)
29. Chai, Y., Xiong, X., Yue, L., Jiang, Y., Pan, Y., Fang, X.: Intramolecular halogen transfer via halonium ion intermediates in the gas phase. J. Am. Soc. Mass Spectrom. **27**, 1–7 (2016)
30. Gal, J.F., Herreros, M., Maria, P.C., Operti, L., Pettigiani, C., Rabezzana, R., Vaglio, G.A.: Gas-phase ion–molecule reactions in organophosphorus esters. J. Mass Spectrom. **34**, 1296–1302 (1999)

31. Liu, D.Q.: Collision-induced fluorine atom migration in atmospheric pressure ionization mass spectrometry. J. Mass Spectrom. **38**, 1210–1212 (2003)

32. Matsubara, H., Ryu, I., Schiesser, C.H.: An ab initio and DFT study of some halogen atom transfer reactions from alkyl groups to acyl radical. Org. Biomol. Chem. **5**, 3320–3324 (2007)

33. Picazas-Márquez, N., Sierra, M., Nova, C., Moreno, J.M., Aboitiz, N., Rivas, G.D., Sierra, M.A., Martínez-Álvarez, R., Gómez-Caballero, E.: GC-MS study of mono- and bishaloethylphosphonates related to schedule 2.B.04 of the chemical weapons convention: the discovery of a new intramolecular halogen transfer. J. Am. Soc. Mass Spectrom. **27**, 1–10 (2016)

34. Stevens, C.V., Van, M.E., Eeckhout, Y., Vanderhoydonck, B., Hooghe, W.: Synthesis of highly functionalised spiro-indoles by a halogen atom transfer radical cyclization. ChemInform **37**, 4827–4829 (2006)

35. Tajima, S., Ueki, M., Tajima, S., Sekiguchi, O., Shigihara, A.: Unimolecular HF loss from the molecular ions of fluorophenols and fluoroanilines. A 'ring-walk' mechanism of a fluorine atom. Rapid Commun. Mass Spectrom. **10**, 1076–1078 (1996)

36. Wang, H.Y., Gao, Y., Zhang, F., Yu, C.T., Xu, C., Guo, Y.L.: Mass spectrometric study of the gas-phase difluorocarbene expulsion of polyfluorophenyl cations via F-atom migration. J. Am. Soc. Mass Spectrom. **24**, 1919–1926 (2013)

37. Zhang, S., Zhu, Z., Ding, Y.: Proposal for halogen atom transfer mechanism for Ullmann O-arylation of phenols with aryl halides. Dalton Trans. **41**, 13832–13840 (2012)

38. Acosta-Tejada, G.M., Medina-Peralta, S., Moguel-Ordonez, Y.B., Munoz-Rodriguez, D.: Matrix solid-phase dispersion extraction of organophosphorus pesticides from propolis extracts and recovery evaluation by GC/MS. Anal. Bioanal. Chem. **400**, 885–891 (2011)

39. Chen, Y.I., Su, Y.S., Jen, J.F.: Determination of dichlorvos by on-line microwave-assisted extraction coupled to headspace solid-phase microextraction and gas chromatography-electron-capture detection. J. Chromatogr. A **976**, 349–355 (2002)

40. Sanusi, A., Ferrari, F., Millet, M., Montury, M.: Pesticide vapors in confined atmospheres. Determination of dichlorvos by SPME-GC-MS at the μg m–3 level. J. Environ. Monit. **5**, 574–577 (2003)

41. Schultz, D.R., Marxmiller, R.L., Koos, B.A.: Residue determination of dichlorvos and related metabolites in animal tissue and fluids. J. Agric. Food Chem. **19**, 1238–1243 (1971)

42. Tuoro, D.D., Portaccio, M., Lepore, M., Arduini, F., Moscone, D., Bencivenga, U., Mita, D.G.: An acetylcholinesterase biosensor for determination of low concentrations of paraoxon and dichlorvos. New Biotechnol. **29**, 132–138 (2011)

43. Wang, G.M., Dai, H., Li, Y.G., Li, X.L., Zhang, J.Z., Zhang, L., Fu, Y.Y., Li, Z.G.: Simultaneous determination of residues of trichlorfon and dichlorvos in animal tissues by LC-MS/MS. Food Addit. Contam. **27**, 983–988 (2010)

44. Wang, J., Zhang, C., Wang, H., Yang, F., Zhang, X.: Development of a luminol-based chemiluminescence flow-injection method for the determination of dichlorvos pesticide. Talanta **54**, 1185–1193 (2001)

45. Morizur, J.P., Taphanel, M.H., Gevrey, S., Bouguerra, M.L., Driss, M.R.: Analytical study of dichlorvos by mass spectrometry: evidence for ion/molecule reactions. Analusis **24**, 177–181 (1996)

46. Kotek, V., Dvořáková, H., Tobrman, T.: Modular and highly stereoselective approach to all-carbon tetrasubstituted alkenes. Org. Lett. **17**, 608–611 (2015)

47. Frisch, M., Trucks, G.W., Schlegel, H.B., Scuseria, G.E., Robb, M.A., Cheeseman, J.R., Zakrzewski, V.G., Montgomery, J.A., Jr., R.E.S., Burant, J.C., Dapprich, S., Millam, J.M., Daniels, A.D., Kudin, K.N., Strain, M.C., Farkas, O., Tomasi, J., Barone, V., Cossi, M., Cammi, R., Mennucci, B., Pomelli, C., Adamo, C., Clifford, S., Ochterski, J., Petersson, G.A., Ayala, P.Y., Cui, Q., Morokuma, K., Malick, D.K., Rabuck, A.D., Raghavachari, K., Foresman, J.B., Cioslowski, J., Ortiz, J.V., Stefanov, B.B., Liu, G., Liashenko, A., Piskorz, P., Komaromi, I., Gomperts, R., Martin, R.L., Fox, D.J., Keith, T., Al-Laham, M.A., Peng, C.Y., Nanayakkara, A., Gonzalez, C., Challacombe, M., Gill, P.M.W., Johnson, B., Chen, W., Wong, M.W., Andres, J.L., Gonzalez, C., Head-Gordon, M.E., Replogle, S., Pople., J.A.: Gaussian 03, Revision B.03, Gaussian, Inc.: Wallingford (2004)

48. Purna Chander, C., Raju, G., Mathai, G., Srinivas, R., Gaikwad, H.K., Bantu, R., Nagarapu, L.: Electrospray ionization tandem mass spectrometry of 3-phenyl-N-(3-(4-phenylpiperazin-1-yl)propyl)-1H-pyrazole- 5-carboxamide derivatives: unusual fragmentation involving loss of 11 u. Rapid Commun. Mass Spectrom. **26**, 207–214 (2012)

49. Guo, C., Jiang, K., Yue, L., Xia, Z., Wang, X., Pan, Y.: Intriguing roles of reactive intermediates in dissociation chemistry of N-phenylcinnamides. Org. Biomol. Chem. **10**, 7070–7077 (2012)